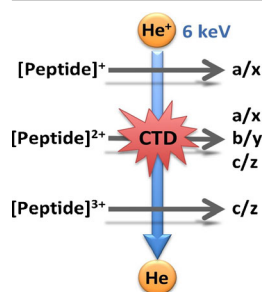


Charge Transfer Dissociation (CTD) Mass Spectrometry of Peptide Cations: Study of Charge State Effects and Side-Chain Losses

Pengfei Li,¹ Glen P. Jackson^{1,2}

¹C. Eugene Bennett Department of Chemistry, West Virginia University, Morgantown, WV 26506, USA

²Department of Forensic and Investigative Science, West Virginia University, Morgantown, WV 26506-6121, USA



Abstract. 1+, 2+, and 3+ precursors of substance P and bradykinin were subjected to helium cation irradiation in a 3D ion trap mass spectrometer. Charge exchange with the helium cations produces a variety of fragment ions, the number and type of which are dependent on the charge state of the precursor ions. For 1+ peptide precursors, fragmentation is generally restricted to C–CO backbone bonds (*a* and *x* ions), whereas for 2+ and 3+ peptide precursors, all three backbone bonds (C–CO, C–N, and N–C α) are cleaved. The type of backbone bond cleavage is indicative of possible dissociation channels involved in CTD process, including high-energy, kinetic-based, and ETD-like pathways. In addition to backbone cleavages, amino acid side-chain cleavages are observed in CTD, which are consistent with other high-energy and

radical-mediated techniques. The unique dissociation pattern and supplementary information available from side-chain cleavages make CTD a potentially useful activation method for the structural study of gas-phase biomolecules.

Keywords: Radical ion, Peptide fragmentation, Ion/ion reaction, Charge transfer, Electron transfer

Received: 19 August 2016/Revised: 3 December 2016/Accepted: 4 December 2016/Published Online: 13 January 2017

Introduction

In recent years, mass spectrometry (MS) has become an indispensable tool for the study of biological molecules such as lipids [1], oligosaccharides [2], peptides [3, 4], proteins [5], and DNA [6]. With the development of soft ionization methods such as fast atom bombardment (FAB), matrix-assisted laser desorption/ionization (MALDI), and electrospray ionization (ESI), single-stage MS plays an important role in the molecular weight determination of an intact molecule of interest [7]. However, interrogation of detailed structural information of a gas-phase molecule usually requires multiple stages of MS or tandem mass spectrometry (MS/MS) [8].

A variety of MS/MS fragmentation methods have been developed and implemented on modern mass spectrometric

instruments, the most common of which is collision-induced dissociation (CID) [9]. Collisional activation tends to break the weakest bonds of gas-phase peptides and proteins—such as amide bonds—and produces *b/y* ions for the deduction of peptide sequence information. However, CID can also result in the loss of weakly bound post-translational modifications (PTMs), which has been shown to limit its usefulness [10, 11].

Electron capture and electron transfer dissociation (ECD/ETD or ExD) are two alternative MS/MS techniques that can overcome the aforementioned limitations [12]. Unlike CID, ExD cleaves peptide backbone N–C α bonds to produce *c/z* ions with a more extensive peptide/protein sequence coverage than CID [13]. In addition, ExD retains PTMs to a much greater extent than CID, which facilitates the elucidation of PTM site information [12]. However, the fact that ExD relies on charge reduction makes it incompatible with 1+ precursor ions, and its performance is compromised for 2+ precursor ions [14]. The inefficiency with peptide dications can be problematic for implementing ExD with enzymatic digestion workflows because many tryptically digested peptides are doubly charged [15].

Electronic supplementary material The online version of this article (doi:10.1007/s13361-016-1574-y) contains supplementary material, which is available to authorized users.

Correspondence to: Glen P. Jackson; e-mail: glen.jackson@mail.wvu.edu

To combat these issues, significant interest has been placed in the development of new ion activation methods, such as electronic excitation dissociation (EED) [16], electron ionization dissociation (EID) [17], ultraviolet photodissociation (UVPD) [18, 19], femtosecond laser-induced ionization/dissociation (fs-LID) [20], action spectroscopy (synchrotron radiation) [21], and metastable atom-activated dissociation (MAD) [22, 23]. These fragmentation methods all possess a common feature—the capability of dissociating low charge state ($1+$ & $2+$) precursor ions, thus providing complementary structural information to ETD/ECD. Some methods (e.g., EID) even show almost equal fragmentation efficiency and sequence coverage between the dissociation of $1+$, $2+$, and multiply charged precursor ions [17], which makes them promising for a proteomic workflow.

Charge transfer dissociation (CTD) is another alternative ion activation method for MS/MS experiments [24]. Contrary to the common ion/ion dissociation methods, CTD utilizes the interaction between homo-polarity ions such as peptide cations and helium cations, which, in the case of $1+$ substance P, results in a dominant series of a ions. It has been widely reported that the fragmentation pattern of MS/MS techniques shows certain dependence on the charge state of precursor ions and the type of mass analyzer [14, 19, 25]. To investigate this dependence, CTD fragmentation of substance P and bradykinin at different charge states ($1+$, $2+$, and $3+$) was carried out in a 3D ion trap mass spectrometer. Various types of cleavages were observed—including backbone and side-chain cleavages—which provide mechanistic insight into the fragmentation channels involved in CTD process. Although our preliminary studies were conducted on a 2D ion trap [24], the current work was accomplished on a 3D ion trap, which shows some subtle differences in the resulting fragmentation patterns. The somewhat improved capabilities of the current 3D trap configuration probably stem from the closer proximity between the helium ion gun and the trapping volume.

Experimental

Instrumentation

He-CTD fragmentations of substance P and bradykinin were carried out using a modified Bruker amaZon ETD mass spectrometer (Bruker Daltonics, Bremen, Germany). A saddle field ion/fast atom source (VSW/Atomtech, Macclesfield, UK) installed with the ion gun anode lens was interfaced onto the top cover of 3D ion trap via a home-built metal cover [24]. The source installation, connection between electronic components, and the working principle are similar to our previous instrumental setup on LTQ Velos Pro and experimental setup of MAD-MS [9, 24].

Reagents

Substance P and bradykinin were purchased from Sigma-Aldrich (St. Louis, MO, USA) and used without further purification. The peptides were reconstituted into a water/

methanol/acetic acid mixture (49.5:49.5:1 v/v/v), aiming for a final concentration of $60\ \mu\text{M}$, and were electrosprayed using a standard (Bruker, Billerica, MA) Apollo source [9].

Method

Experiments were performed in the MS/MS mode on the 3D ion trap instrument, and the saddle field ion source was switched on during the section of scan function that is typically reserved for CID. The peptide solutions were infused using an electronic syringe pump (#1725; Hamilton Company, Reno, NV, USA) at a flow rate of $160\ \mu\text{L/h}$. Precursor ions were isolated using an isolation window of $2\ \text{Da}$, after which they were irradiated with the helium cation beam. The low mass cut-off (LMCO) value was typically set to be $m/z\ 150$ for the removal of ionized pump oil fragments. A $+6\ \text{kV}$ square wave with a pulse width of $25\ \text{ms}$ was supplied to the saddle field ion source anode for the generation of reagent helium cations. The helium gas flow was controlled via a variable leak valve, and the pressure read-out was obtained from the ion trap gauge in the main vacuum region. Using this indirect measurement, the helium gas supply was adjusted to provide a main vacuum pressure of $\sim 1.20 \times 10^{-5}\ \text{mbar}$ for all the experiments, which is only slightly above the base pressure around $8 \times 10^{-6}\ \text{mbar}$. All the CTD mass spectra presented in this work were time-averaged for $0.5\text{--}2\ \text{min}$ to improve the signal-to-noise ratio (S/N).

Results and Discussion

Helium CTD (He-CTD) was performed on singly, doubly, and triply protonated Substance P, respectively, as shown in Figure 2. Upon the interaction with helium cations, the $1+$, $2+$, and $3+$ precursors of substance P gave oxidized product ions (charge-increased species) at $m/z\ 673.9$, 450.4 , and 337.8 , corresponding to product ions $[\text{M} + \text{H}]^{2+}$, $[\text{M} + 2\text{H}]^{3+}$ and $[\text{M} + 3\text{H}]^{4+}$, respectively. Gas-phase oxidation, or increasing the charge state of gas-phase ions has been observed in a variety of fragmentation methods, including He-MAD [9, 26], EID and EED [16, 17], and photon-based dissociation methods [20, 21].

Charge-increased species mainly originate from the electron detachment of precursor ions, i.e. charge transfer. Helium cations have an electron affinity of $\sim 24.6\ \text{eV}$, and given that they are generated from a $6\ \text{kV}$ saddle field ion source, there is more than enough energy to overcome the Coulombic repulsion barrier to enable charge transfer to occur [8, 21, 24, 26, 27]. In addition to the charge-increased species, charge-reduced product ions were observed in He-CTD spectra of $2+$ and $3+$ substance P cations. These hydrogen-rich charge-reduced species correspond to $m/z\ 1349.8$ ($[\text{M} + 2\text{H}]^{+}$) and $m/z\ 675.0$ ($[\text{M} + 3\text{H}]^{2+}$) respectively, which are commonly observed in electron-based methods (e.g., ECD/ETD). It seems unreasonable for He^+ to serve as an electron transfer reagent for such charge reduction reactions, so we performed several

experiments to investigate the source of the electron-donating reagents.

Despite the fact that the CTD source is designed to operate as an efficient cation source, a wide range of negative ions are observed in the background CTD spectrum when the trap is operated in negative ion mode (see [Supplemental Material](#) for details). Although we are unsure of the exact mechanism(s) of negative ion formation, the CTD source is apparently able to form negative ions from background impurities in the trap, and these anions can be trapped and used as reagent anions for ETD. One of the more abundant background ions has a mass-to-charge ratio of 184 (see [Supplementary Figure S2](#), for example), does not fragment using CID, and reacts with residual oxygen to form adducts at $M + 16$ (m/z 200) and $M + 32$ (m/z 216). CID of the $M + 16$ and $M + 32$ adducts re-forms the original reagent anion at m/z 184, indicating that the reagent is probably polycyclic/aromatic and almost certainly a radical (*vide infra*) [28–30].

Figure 1c shows that these reagent anions are reasonably effective at forming c and z ions from the 3+ precursor of substance P. Fortunately, this charge reduction mechanism can be minimized by raising the LMCO during CTD activation to prevent the co-accumulation of reagent anions, with the caveat that increasing the LMCO also limits the observable range of product ions for CTD. The same CTD experiment with an elevated LMCO is shown in [Supplementary Figure S5](#). The intensity of charge-reduced species $[M + 2H]^{++}$ decreased dramatically with increasing LMCO, with no significant change in the intensity of other product ions.

A series of a ions was observed in the He-CTD spectrum of singly protonated substance P, which is consistent with our previous experimental results on a 2D ion trap [24]. The current work shows additional low-mass fragment ions (e.g., a_2 , b_2 , and c_2) that were not observed on the 2D ion trap, but weaker signal-to-noise (S/N) for fragments in the range from m/z 700 to 1300. Reilly et al. [19] have reported that the fragmentation of ions observed in UV photodissociation can be affected by the type of mass analyzer, and we suspect that the observed

differences between the 2D trap results and 3D trap results are caused by experimental differences. These differences could be minimized by raising the LMCO value and increasing the CTD time on the 3D ion trap to make the conditions more similar to the experiments on the 2D ion trap.

Similar to electron-based fragmentation methods [14, 25], CTD of substance P also shows certain charge state-dependence on fragmentation. Product ion spectra of He-CTD of 2+ and 3+ substance P produced more than twice the number of fragment ions than the 1+ precursor, mainly because of the addition of c and z ions. Additional doubly and triply charged fragment ions were also observed from the higher charge state precursor ions. For example, the He-CTD spectrum of 2+ substance P (Figure 2b) is dominated by both a and b ions, with a few c , y , and z ions, but the He-CTD spectrum of 3+ substance P is dominated by c ions. The near-complete series of a ions for the 1+ precursor is commonly observed in high-energy dissociation methods, and suggests the involvement of a high-energy fragmentation channel [24]. The existence of b/y and c/z fragment ion series mainly originates from vibrational excitation (e.g., CID) and charge-reduction processes, respectively, which clearly become more dominant than oxidation as the charge state of the precursor increases.

To probe the relationship between CTD and ETD, ETD fragmentation of 2+ and 3+ substance P was conducted on the same instrument. Results are provided in the [Supplemental Material](#) ([Supplementary Figure S1](#)). ETD of 2+ substance P produced only six c ions, covering half of the peptide sequence. In contrast, ETD of 3+ substance P produced almost complete sequence coverage of c ions, along with some a , b , and z ions.

In addition to the aforementioned backbone fragmentation, side-chain cleavages were observed for substance P, as shown in Figures 3 and 4. Amino acid side-chain losses have been well-noted and referred to as $(M^* - X)$ regions in variety of tandem MS approaches, including UVPD [18, 19], action spectroscopy [21], fs-LID [20], EID [17], EED [16], ECD [31–38], ETD [39], CID [40], and MAD [9].

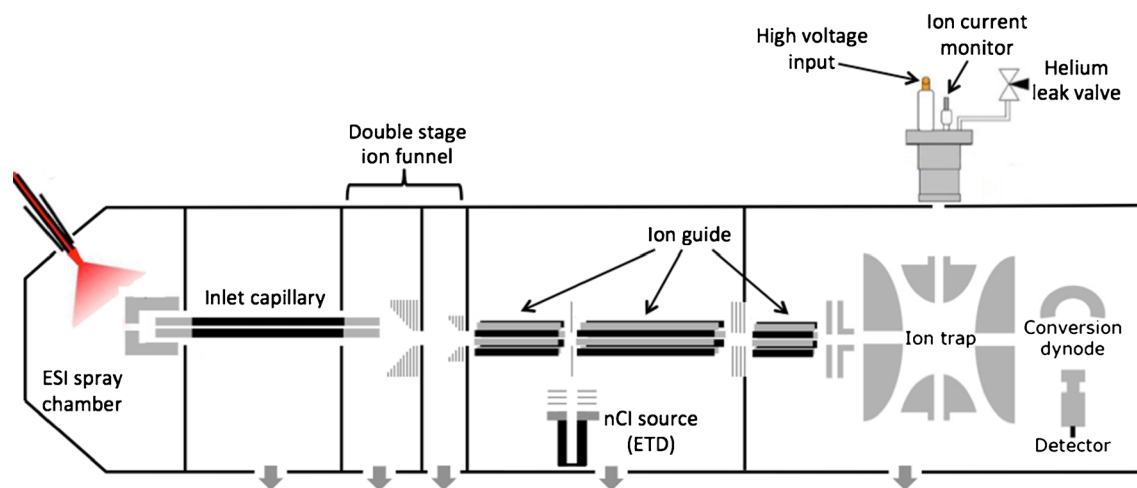


Figure 1. Schematic of installation of saddle field ion source onto Bruker amaZon ETD mass spectrometer

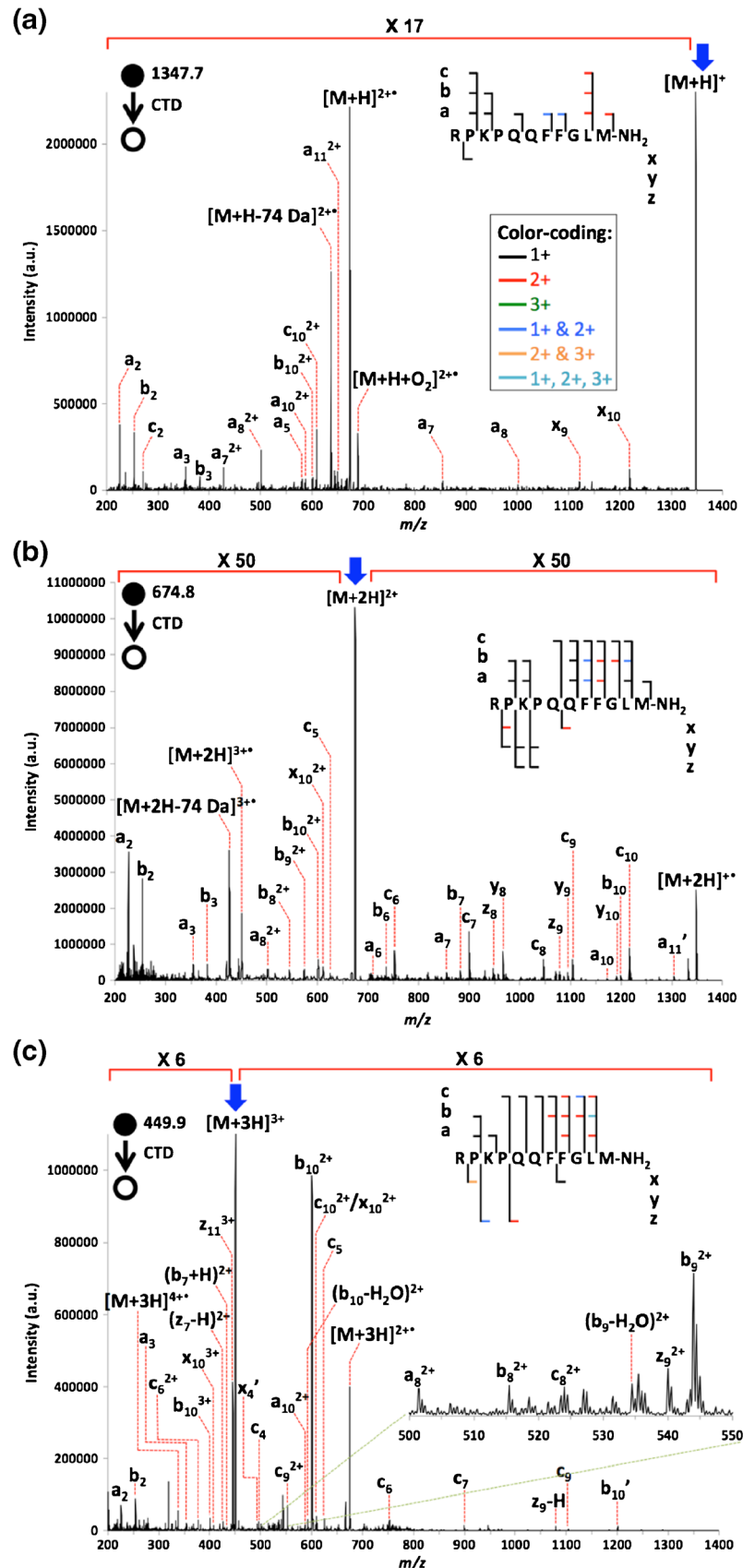


Figure 2. He-CTD spectrum of (a) singly, (b) doubly, and (c) triply protonated substance P. The m/z ranges of interest have been multiplied by factors of 17, 50, and 6, respectively, for clarity. Precursor ions are indicated by blue arrows. The inset in panel (a) shows the color-coding scheme of peptide sequencing used throughout this work

Figure 3 provides zoomed-in regions of the same spectra from Figure 2 to show more clearly the side-chain losses from the ionized product ions. The oxidized cations are often referred to as hydrogen-deficient species in other studies [17]. For the He-CTD spectrum of 1+ substance P, diagnostic side-chain losses from $[M + H]^{2+}$ were observed, including even-electron rearrangements and radical losses. These observations are consistent with commonly-observed neutral losses from $[M + H]^{2+}$, including: 1 Da ($\cdot H$) [17], 15 Da ($\cdot CH_3$ from Met) [21], 47 Da ($\cdot SCH_3$ from Met) [21], 58 Da ($\cdot CH_2CONH_2$ from Glu) [21, 40], 61 Da ($\cdot CH_2SCH_3$ from Met) [8], 71 Da ($CH_2 = CHCONH_2$ from Glu) [40], and 74 Da ($CH_2 = CHSCH_3$ from Met) [8, 16].

An interesting ion at m/z 689.9 was also observed and is tentatively assigned as an oxygen adduct of the oxidized product ion (i.e., $[M + H + O_2]^{2+}$). This ion is accompanied by an ion 44 Da less at m/z 667.8, which probably corresponds to $[M + H - CO_2 + O_2]^{2+}$ probably forms from the oxidation of the $[M + H - CO_2]^{2+}$ product [8, 17]. Radical ions have been observed to react with residual oxygen during their confinement in electrodynamic ion traps, which was also noted for the ETD-generated z^{\cdot} ions [28, 29] and MAD-generated $[POPC]^{+\cdot}$ radical ions [30].

When the charge state of substance P precursor increases to 2+ and 3+, fewer side-chain losses from ionized species were observed. Observed losses include: 17 Da (NH_3) [21], 74 Da ($CH_2 = CHSCH_3$ from Met) [16], and 92 Da ($CH_3(C_6H_5)$ from Phe) [21] were lost from $[M+2H]^{3+}$. 17 Da (NH_3) [21], 74 Da ($CH_2 = CHSCH_3$ from Met) [16] and 99 Da ($CH_2 = CH(CH_2)NHC(CH_2) = NH$ from Arg) [40] were lost from $[M + 3H]^{4+}$.

Figure 3a shows CTD of the 1+ precursor ion. In this spectrum, the product ion at m/z 673.4 ($[M]^{2+}$) likely results from an H^{\cdot} loss from the oxidized product ion, $[M + H]^{2+}$, whereas the loss of 1 Da neutrals ($\cdot H$) from charge increased (oxidized) products likely involves the loss of H radicals, the same loss of 1 Da from charge-reduced species, such as in Figure 4a, most likely originating from a competitive proton transfer processes during the reactions.

Zoomed-in m/z regions of charge-reduced species from He-CTD spectra of 2+ and 3+ substance P precursors are shown in top panels of Figure 4a and b. ETD spectra of 2+ and 3+ substance P are magnified to show the $(M^{\cdot} - X)$ regions, which are listed as bottom panels in Figure 4a, b, and an individual panel in Figure 4c.

The CTD spectrum in top panel of Figure 4a shows several neutral losses from $[M + 2H]^{3+}$, including 18 Da (H_2O or $\cdot H + NH_3$) [17, 41–43], 46 Da ($\cdot H + HCONH_2$ from Glu) [41, 42], 60 Da ($\cdot H + \cdot NHC(NH_2) = NH_2^+$ from Arg) [31, 41–43], 75 Da ($\cdot H + CH_2 = CHSCH_3$ from Met) [34, 43], and 101 Da ($\cdot (CH_2)_3NHC(NH_2) = NH_2^+$ from Arg) [34]. Similar neutral losses from the ETD product $[M + 2H]^{3+}$ are also observed [39]. Two exceptions are the 75 Da side-chain loss, which is unique to CTD, and the 29 Da loss, which is only observed in the ETD product ion spectrum. In the absence of high mass accuracy, the 29 Da loss is tentatively assigned as $\cdot H + CO$ [41].

Compared with the low abundance and small neutral losses from the $[M + 2H]^{3+}$ product ion, neutral losses from the $[M + 3H]^{2+}$ product ion are more abundant for both CTD and ETD. Moreover, the types of neutral losses from the radical dication $[M + 3H]^{2+}$ are also different from that of $[M + 2H]^{3+}$. The observed neutral losses in the CTD spectrum and their tentative assignments are: 15 Da ($\cdot CH_3$) [43], 18 Da (H_2O or $\cdot H + NH_3$) [17, 41, 43], 43 Da ($\cdot C(NH_2) = NH$ from Arg or $\cdot C(CH_3)_2$ from Leu) [17, 40], 45 Da ($\cdot H + HCONH_2$ from Glu) [41, 42], 59 Da ($\cdot NHC(NH_2) = NH_2^+$ from Arg or CH_3CONH_2 from Glu) [31, 41–43], 71 Da ($CH_2 = CHCONH_2$ from Glu) [40, 43], 74 Da ($CH_2 = CHSCH_3$ from Met) [40, 43], and 91 Da ($\cdot CH_2(C_6H_5)$) [21]. Interestingly, the CTD spectrum has a unique small loss of 91 Da, and the ETD spectrum has a unique loss of 34 Da $[2(NH_3)]$ from Arg [39].

Unlike CTD, ETD of 3+ Substance P precursor also produced the singly charged ETnoD product ($[M + 3H]^{+\cdot}$), whose $(M^{\cdot} - X)$ region shows the same small losses as those observed for $[M + 2H]^{3+}$ and $[M + 3H]^{2+}$. Similar neutral losses have also been observed in ECD experiments [41].

In general, the CTD and ETD spectra show many similarities in the $(M^{\cdot} - X)$ regions of both $[M + 2H]^{3+}$ and $[M + 3H]^{2+}$. The similar neutral losses between the two activation methods are indicative of similar fragmentation mechanism, which adds more confidence to our previous hypothesis that electron-based fragmentation mainly accounts for the fragments located in the high mass end of CTD spectrum. The similarity in CTD and ETD spectra of multiply charged precursor ions suggests that the ExD-like fragments in CTD experiments originate from the interaction with ETD-like reagent anions, such as negative ions derived from vacuum pump oil or other common contaminants.

By operating the trap in negative ion mode, the CTD source and trap conditions can be shown to produce multiple anions in the region m/z 180–220 (Supplementary Figure S2). One particularly abundant anion exists at m/z 184. Isolation of this abundant background anion showed two interesting properties: (1) the anion could reversibly add O and O_2 , which indicates the anion is a radical; and (2) the anion is resistant to collisional activation, which indicates it may contain fused ring systems. The [Supplemental Materials](#) provide more details about the interrogation of the background anion in CTD. Background anions generated by the CTD gun are present at most m/z values below 200, and they can be easily excluded from the trap to prevent electron transfer reactions by raising the LMCO value >220 Da. Charge reduction (e.g., ETD-like activation) is still observed, even when the co-storage of anions and cations is minimized, which indicates that a second mechanism must also exist to explain the charge reduction of multiply protonated peptide cations. It is possible that the helium cation beam contains a fraction of helium metastable atoms, which have relatively low ionization potentials and could serve as an electron transfer reagents.

He-CTD was also conducted on 1+, 2+, and 3+ bradykinin cations, and the results are shown in Figure 5. Upon irradiation with helium cations, charge-increased product ions were

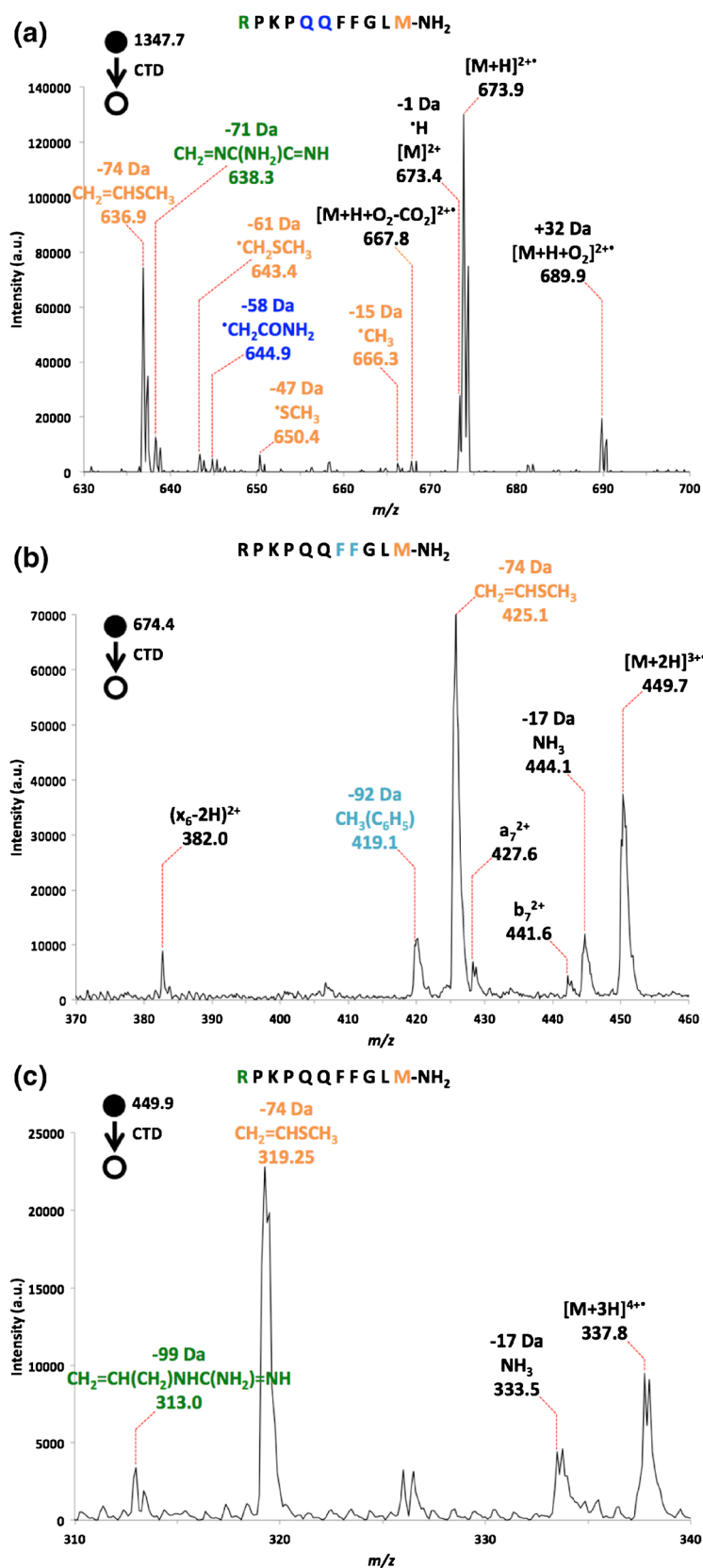


Figure 3. Zoomed-in He-CTD spectra of (a) 1+, (b) 2+, and (c) 3+ precursor ions of substance P, showing m/z ranges corresponding to the $(M^+ - X)$ ranges of oxidized (charge-increased) product ions

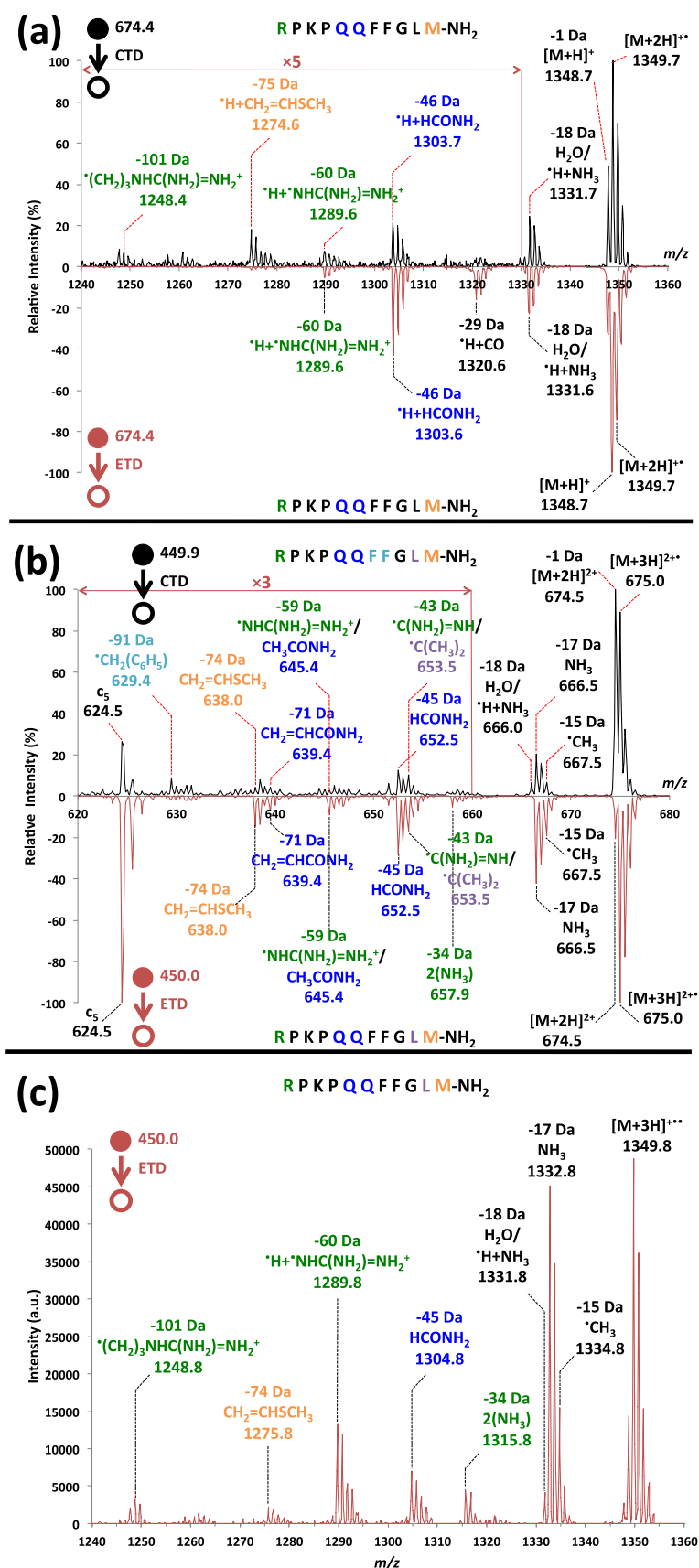


Figure 4. Head-to-tail zoomed-in spectra of reduced (charge-decreased) product ions of (a) He-CTD versus ETD of 2+ Substance P, (b) He-CTD versus ETD of 3+ substance P, and (c) 1+ product ions from ETD of 3+ substance P. Each spectrum is normalized to the tallest peak within the ($M^* - X$) range of charge-reduced product ions

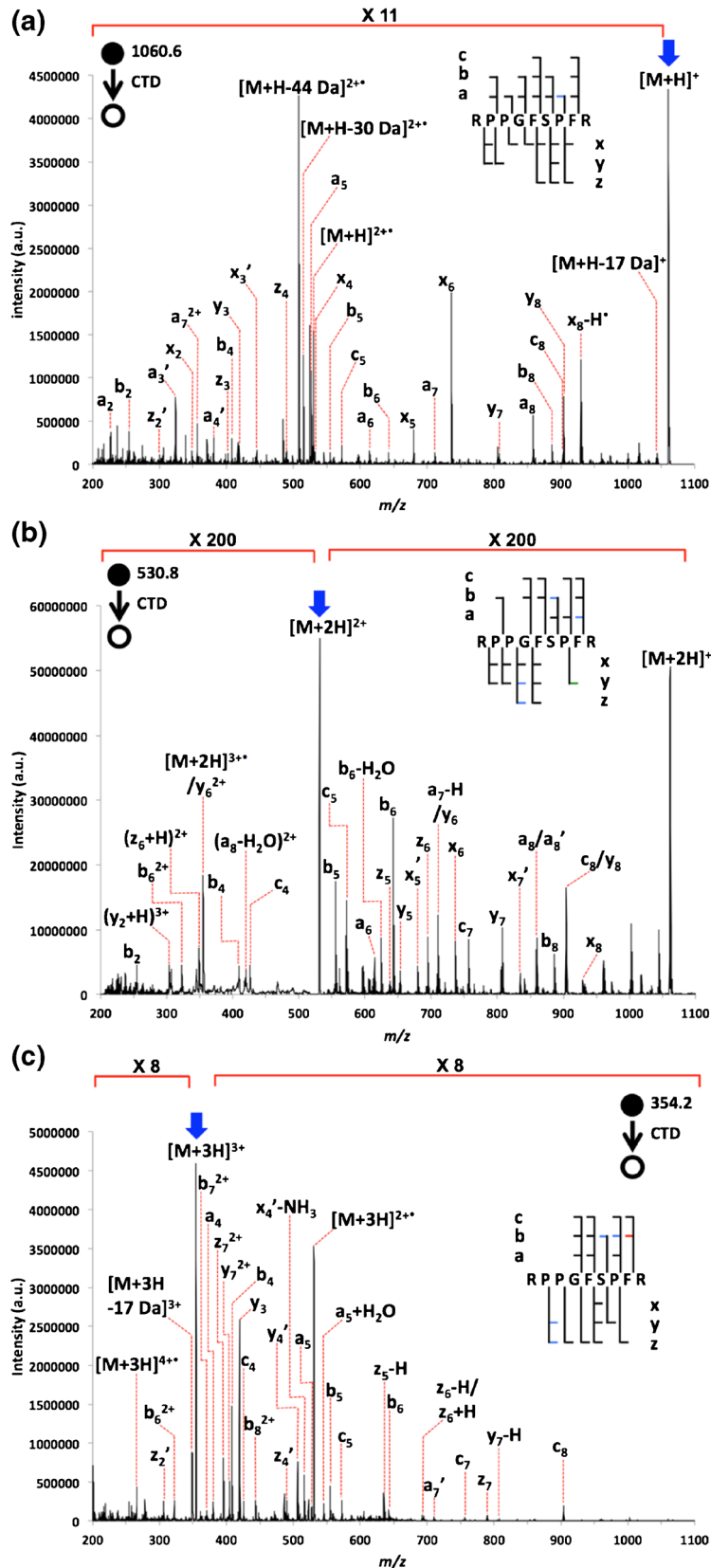


Figure 5. He-CTD spectrum of (a) singly, (b) doubly, and (c) triply protonated bradykinin. Different m/z ranges of interest have been multiplied by a factor of 11, 200, and 8, respectively, for clarity

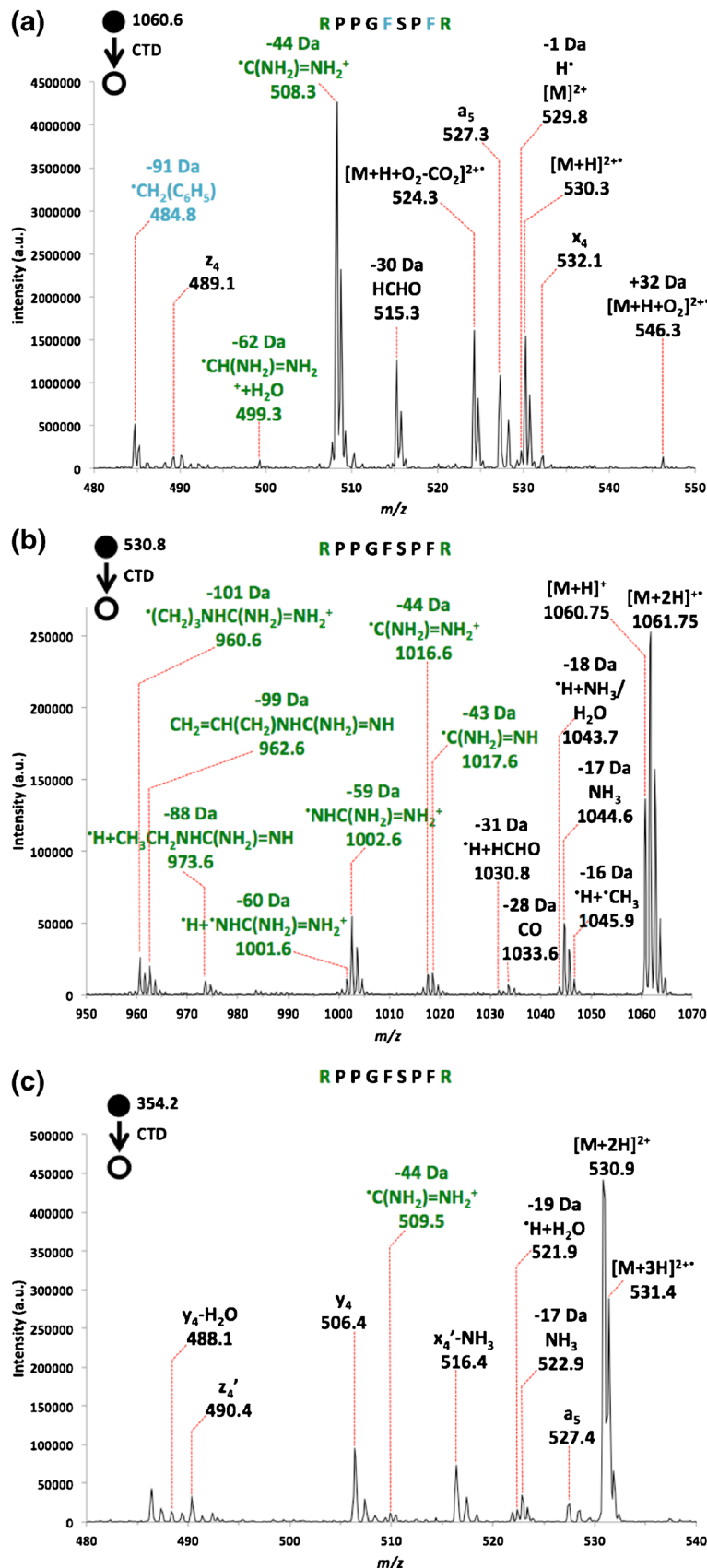


Figure 6. Zoomed-in He-CTD spectra of (a) singly protonated bradykinin showing ($\text{M}^+ - \text{X}$) regions of $[\text{M} + \text{H}]^{2+}$ (oxidized product ion), (b) doubly, and (c) triply protonated bradykinin showing ($\text{M}^+ - \text{X}$) regions of $[\text{M} + 2\text{H}]^{2+}$ and $[\text{M} + 3\text{H}]^{2+}$ (charge-reduced product ions), respectively

observed for all three charge states. Charge-reduced product ions could only be observed for 2+ and 3+ precursors of bradykinin, as expected. These observations are in good agreement with the observations for CTD of substance P [24], and the previous study by Zubarev and coworkers [26]. Unlike CTD of 1+ substance P, CTD of 1+ bradykinin produces an abundant series of *x* ions in addition to the previously observed *a* ions. CTD of 1+ bradykinin also produces more *b*, *y*, *c*, and *z* ions. The coexistence of *a/x* ion pairs provides greater confidence in sequencing and more confidence that the *a* ions are formed via direct C–CO cleavage and not from CO losses from intermediate *b* ions.

Consistent with He-CTD results of 2+ and 3+ substance P, fewer *a/x* ions and more *b/y* and *c/z* ions are observed for 2+ and 3+ bradykinin. Similar to CTD of 3+ substance P, the product ion spectrum for CTD of 3+ bradykinin is dominated by *c/z* ions. The abundant *c/z* ions again point to the domination of an ETD-like mechanism for the higher charge state precursors in CTD.

As shown in Figure 6a, He-CTD of 1+ bradykinin precursor produced five significant fragments corresponding to small neutral losses from $[M + H]^{2+}$. Similar to the ($M^* - X$) regions of substance P, an oxygen adduct ion at *m/z* 546.3 as well as an accompanying ion at *m/z* 524.3 (formed through CO₂ loss) are observed.

As might be expected, significant differences in small neutral losses of bradykinin and substance P are observed. For example, bradykinin in Figure 6a shows four different small losses: 30 Da (HCHO) [17], 44 Da ($\dot{C}(\text{NH}_2) = \text{NH}_2^+$ from Arg) [21], 62 Da ($\dot{C}(\text{NH}_2) = \text{NH}_2^+ + \text{H}_2\text{O}$) [21], and 91 Da ($\dot{\text{C}}\text{H}_2(\text{C}_6\text{H}_5)$ from Phe) [21], two of which are of significantly higher intensity compared with that in CTD experiment of 1+ substance P. The appearance of fragments corresponding to side-chain losses from phenylalanine and arginine in the ($M^* - X$) region of $[M + H]^{2+}$ is consistent with the fact that bradykinin possesses twice the amount of phenylalanine and arginine residues, and that these residues are at or adjacent to the C-terminus in bradykinin.

He-CTD of 2+ and 3+ bradykinin cations produced many small losses within the ($M^* - X$) region of $[M + 2H]^{+}$ (Figure 6b), and a few small losses within the ($M^* - X$) region of $[M + 3H]^{2+}$ (Figure 6c). Most of the small losses for bradykinin are similar to those observed in the same ($M^* - X$) region of charge-reduced species from CTD of 2+ and 3+ of substance P. The similar neutral losses include: 16 Da ($\dot{\text{H}} + \dot{\text{C}}\text{H}_3$), 17 Da (NH₃), 18 Da (H₂O or $\dot{\text{H}} + \text{NH}_3$), 28 Da (CO), 43 Da ($\dot{\text{C}}(\text{NH}_2) = \text{NH}$ from Arg), 59 Da ($\dot{\text{N}}\text{HC}(\text{NH}_2) = \text{NH}_2^+$ from Arg), 101 Da ($\dot{\text{C}}(\text{CH}_2)_3\text{NHC}(\text{NH}_2) = \text{NH}_2^+$ from Arg). Different small losses are observed as well. For example, bradykinin shows losses corresponding to: 19 Da ($\dot{\text{H}} + \text{H}_2\text{O}$) [43], 31 Da ($\dot{\text{H}} + \text{HCHO}$) [17], 44 Da ($\dot{\text{C}}(\text{NH}_2) = \text{NH}_2^+$ from Arg) [43], 60 Da ($\dot{\text{H}} + \dot{\text{N}}\text{HC}(\text{NH}_2) = \text{NH}_2^+$ from Arg) [39], 88 Da ($\dot{\text{H}} + \text{CH}_3\text{CH}_2\text{NHC}(\text{NH}_2) = \text{NH}$ from Arg) [43], and 99 Da ($\text{CH}_2 = \text{CH}(\text{CH}_2)\text{NHC}(\text{NH}_2) = \text{NH}$ from Arg) [41]. Compared with substance P (RPKPQQFFGLM), bradykinin (RPPGFSPFR) has a higher composition of arginine residues, which could

possibly account for the more frequent observation of arginine side-chain losses in bradykinin. A similar observation was observed in the ECD study of bradykinin methyl ester (RPPGFSPFROCH₃) [41]. Upon ECD, bradykinin with a C-terminal methylester showed a predominance of arginine-specific losses in the ($M^* - X$) region of $[M + 2H]^{+}$.

Conclusions

Charge transfer dissociation of singly, doubly, and triply protonated substance P and bradykinin was conducted in a 3D ion trap mass spectrometer. The charge state of the precursor ions significantly impacted the number and the types of ions produced—*a/x* versus *c/z*—correlating with the relative contributions of oxidative versus reductive mechanisms, respectively. Consistent with our previous experimental results, CTD of singly charged precursors produces an abundance of *a/x* fragments, and the distribution of charge between complementary *a/x* ion pairs is dependent on the relative basicity of the peptide termini. CTD of doubly and triply charged precursors produced additional *b/y* ions and *c/z* ions. The type of fragment ions provides helpful hints on possible fragmentation channels that CTD adopts: high-energy and ETD-like (i.e., radical) pathways. Accompanying side-chain losses were also observed in CTD spectra, which are in good agreement with the previous results from photo-activated, collisionally activated, and electron-based dissociation experiments. The side-chain losses can provide valuable diagnostic information about amino acid composition to support the backbone-sequencing ions. The enriched structural information obtainable via CTD, along with the relative low-cost of 3D ion instrument platform, makes this approach a promising tool for the interrogation of gas-phase biomolecules.

Acknowledgments

The authors acknowledge financial support from the National Institutes of Health (NIH) (1R01GM114494-01). The opinions, findings, and conclusions or recommendations expressed in this publication are those of the author(s) and do not necessarily reflect the views of NIH.

References

1. Lee, H., An, H.J., Lerno, L.A., German, J.B., Lebrilla, C.B.: Rapid profiling of bovine and human milk gangliosides by matrix-assisted laser desorption/ionization Fourier transform ion cyclotron resonance mass spectrometry. *Int. J. Mass Spectrom.* **305**(2/3), 138–150 (2011)
2. Ko, B.J., Brodbelt, J.S.: 193 nm ultraviolet photodissociation of deprotonated sialylated oligosaccharides. *Anal. Chem.* **83**(21), 8192–8200 (2011)
3. Lopez-Clavijo, A.F., Duque-Daza, C.A., Creese, A.J., Cooper, H.J.: Electron capture dissociation mass spectrometry of phosphopeptides: arginine and phosphoserine. *Int. J. Mass Spectrom.* **390**, 63–70 (2015)
4. Voinov, V.G., Hoffman, P.D., Bennett, S.E., Beckman, J.S., Barofsky, D.F.: Electron capture dissociation of sodium-adducted peptides on a modified quadrupole/time-of-flight mass spectrometer. *J. Am. Soc. Mass Spectrom.* **26**(12), 2096–2104 (2015)

5. Lu, J., Trmka, M.J., Roh, S.H., Robinson, P.J.J., Shiao, C., Fujimori, D.G., Chiu, W., Burlingame, A.L., Guan, S.H.: Improved peak detection and deconvolution of native electrospray mass spectra from large protein complexes. *J. Am. Soc. Mass Spectrom.* **26**(12), 2141–2151 (2015)
6. Flett, F.J., Walton, J.G.A., Mackay, C.L., Interthal, H.: Click chemistry generated model DNA-peptide heteroconjugates as tools for mass spectrometry. *Anal. Chem.* **87**(19), 9595–9599 (2015)
7. Sleno, L., Volmer, D.A.: Ion activation methods for tandem mass spectrometry. *J. Mass Spectrom.* **39**(10), 1091–1112 (2004)
8. Kalcic, C.L., Reid, G.E., Lozovoy, V.V., Dantus, M.: Mechanism elucidation for nonstochastic femtosecond laser-induced ionization/dissociation: from amino acids to peptides. *J. Phys. Chem. A* **116**(11), 2764–2774 (2012)
9. Cook, S.L., Collin, O.L., Jackson, G.P.: Metastable atom-activated dissociation mass spectrometry: leucine/isoleucine differentiation and ring cleavage of proline residues. *J. Mass Spectrom.* **44**(8), 1211–1223 (2009)
10. Cook, S.L., Jackson, G.P.: Characterization of tyrosine nitration and cysteine nitrosylation modifications by metastable atom-activation dissociation mass spectrometry. *J. Am. Soc. Mass Spectrom.* **22**(2), 221–232 (2011)
11. Cook, S.L., Jackson, G.P.: Metastable atom-activated dissociation mass spectrometry of phosphorylated and sulfonated peptides in negative ion mode. *J. Am. Soc. Mass Spectrom.* **22**(6), 1088–1099 (2011)
12. Zhurov, K.O., Fornelli, L., Wodrich, M.D., Laskay, U.A., Tsybin, Y.O.: Principles of electron capture and transfer dissociation mass spectrometry applied to peptide and protein structure analysis. *Chem. Soc. Rev.* **42**(12), 5014–5030 (2013)
13. Yoo, H.J., Wang, N., Zhuang, S.Y., Song, H.T., Hakansson, K.: Negative-ion electron capture dissociation: radical-driven fragmentation of charge-increased gaseous peptide anions. *J. Am. Chem. Soc.* **133**(42), 16790–16793 (2011)
14. Liu, J., McLuckey, S.A.: Electron transfer dissociation: effects of cation charge state on product partitioning in ion/ion electron transfer to multiply protonated polypeptides. *Int. J. Mass Spectrom.* **330**, 174–181 (2012)
15. Kjeldsen, F., Giessing, A.M.B., Ingrell, C.R., Jensen, O.N.: Peptide sequencing and characterization of post-translational modifications by enhanced ion-charging and liquid chromatography electron-transfer dissociation tandem mass spectrometry. *Anal. Chem.* **79**(24), 9243–9252 (2007)
16. Nielsen, M.L., Budnik, B.A., Haselmann, K.F., Zubarev, R.A.: Tandem MALDI/EL ionization for tandem Fourier transform ion cyclotron resonance mass spectrometry of polypeptides. *Int. J. Mass Spectrom.* **226**(1), 181–187 (2003)
17. Fung, Y.M.E., Adams, C.M., Zubarev, R.A.: Electron ionization dissociation of singly and multiply charged peptides. *J. Am. Chem. Soc.* **131**(29), 9977–9985 (2009)
18. Barbacci, D.C., Russell, D.H.: Sequence and side-chain specific photofragment (193 nm) ions from protonated Substance P by matrix-assisted laser desorption ionization time-of-flight mass spectrometry. *J. Am. Soc. Mass Spectrom.* **10**(10), 1038–1040 (1999)
19. Thompson, M.S., Cui, W., Reilly, J.P.: Factors that impact the vacuum ultraviolet photofragmentation of peptide ions. *J. Am. Soc. Mass Spectrom.* **18**(8), 1439–1452 (2007)
20. Kalcic, C.L., Gunaratne, T.C., Jonest, A.D., Dantus, M., Reid, G.E.: Femtosecond laser-induced ionization/dissociation of protonated peptides. *J. Am. Chem. Soc.* **131**(3), 940–942 (2009)
21. Canon, F., Milosavljevic, A.R., Nahon, L., Giuliani, A.: Action spectroscopy of a protonated peptide in the ultraviolet range. *Phys. Chem. Chem. Phys.* **17**(39), 25725–25733 (2015)
22. Misharin, A.S., Silivra, O.A., Kjeldsen, F., Zubarev, R.A.: Dissociation of peptide ions by fast atom bombardment in a quadrupole ion trap. *Rapid Commun. Mass Spectrom.* **19**(15), 2163–2171 (2005)
23. Berkout, V.D.: Fragmentation of protonated peptide ions via interaction with metastable atoms. *Anal. Chem.* **78**(9), 3055–3061 (2006)
24. Hoffmann, W.D., Jackson, G.P.: Charge transfer dissociation (CTD) mass spectrometry of peptide cations using kiloelectronvolt helium cations. *J. Am. Soc. Mass Spectrom.* **25**(11), 1939–1943 (2014)
25. Pitteri, S.J., Chrisman, P.A., Hogan, J.M., McLuckey, S.A.: Electron transfer ion/ion reactions in a three-dimensional quadrupole ion trap: reactions of doubly and triply protonated peptides with SO₂ center dot. *Anal. Chem.* **77**(6), 1831–1839 (2005)
26. Chingin, K., Makarov, A., Denisov, E., Rebrov, O., Zubarev, R.A.: Fragmentation of positively-charged biological ions activated with a beam of high-energy cations. *Anal. Chem.* **86**(1), 372–379 (2014)
27. Budnik, B.A., Tsybin, Y.O., Hakansson, P., Zubarev, R.A.: Ionization energies of multiply protonated polypeptides obtained by tandem ionization in Fourier transform mass spectrometers. *J. Mass Spectrom.* **37**(11), 1141–1144 (2002)
28. Xia, Y., Chrisman, P.A., Pitteri, S.J., Erickson, D.E., McLuckey, S.A.: Ion/molecule reactions of cation radicals formed from protonated polypeptides via gas-phase ion/ion electron transfer. *J. Am. Chem. Soc.* **128**(36), 11792–11798 (2006)
29. Smith, S.A., Kalcic, C.L., Safran, K.A., Stemmer, P.M., Dantus, M., Reid, G.E.: Enhanced characterization of singly protonated phosphopeptide ions by femtosecond laser-induced ionization/dissociation tandem mass spectrometry (fs-LID-MS/MS). *J. Am. Soc. Mass Spectrom.* **21**(12), 2031–2040 (2010)
30. Li, P., Hoffmann, W.D., Jackson, G.P.: Multistage mass spectrometry of phospholipids using collision-induced dissociation (CID) and metastable atom-activated dissociation (MAD). *Int. J. Mass Spectrom.* **403**, 1–7 (2016)
31. Zubarev, R.A., Kelleher, N.L., McLafferty, F.W.: Electron capture dissociation of multiply charged protein cations. A nonergodic process. *J. Am. Chem. Soc.* **120**(13), 3265–3266 (1998)
32. Axelsson, J., Palmblad, M., Hakansson, K., Hakansson, P.: Electron capture dissociation of Substance P using a commercially available Fourier transform ion cyclotron resonance mass spectrometer. *Rapid Commun. Mass Spectrom.* **13**(6), 474–477 (1999)
33. Leymarie, N., Costello, C.E., O'Connor, P.B.: Electron capture dissociation initiates a free radical reaction cascade. *J. Am. Chem. Soc.* **125**(29), 8949–8958 (2003)
34. Chalkley, R.J., Brinkworth, C.S., Burlingame, A.L.: Side-chain fragmentation of alkylated cysteine residues in electron capture dissociation mass spectrometry. *J. Am. Soc. Mass Spectrom.* **17**(9), 1271–1274 (2006)
35. Savitski, M.M., Nielsen, M.L., Zubarev, R.A.: Side-chain losses in electron capture dissociation to improve peptide identification. *Anal. Chem.* **79**(6), 2296–2302 (2007)
36. Falth, M., Savitski, M.M., Nielsen, M.L., Kjeldsen, F., Andren, P.E., Zubarev, R.A.: Analytical utility of small neutral losses from reduced species in electron capture dissociation studied using SwedECD database. *Anal. Chem.* **80**(21), 8089–8094 (2008)
37. Jensen, C.S., Wyer, J.A., Houmoller, J., Hvelplund, P., Nielsen, S.B.: Electron-capture induced dissociation of doubly charged dipeptides: on the neutral losses and N–C- α bond cleavages. *Phys. Chem. Chem. Phys.* **13**(41), 18373–18378 (2011)
38. Kaczorowska, M.A.: Electron capture dissociation and collision induced dissociation behavior of peptides containing methionine, selenomethionine, and oxidized methionine. *Int. J. Mass Spectrom.* **389**, 54–58 (2015)
39. Xia, Q.W., Lee, M.V., Rose, C.M., Marsh, A.J., Hubler, S.L., Wenger, C.D., Coon, J.J.: Characterization and diagnostic value of amino acid side chain neutral losses following electron-transfer dissociation. *J. Am. Soc. Mass Spectrom.* **22**(2), 255–264 (2011)
40. Laskin, J., Yang, Z.B., Ng, C.M.D., Chu, I.K.: Fragmentation of alpha-radical cations of arginine-containing peptides. *J. Am. Soc. Mass Spectrom.* **21**(4), 511–521 (2010)
41. Cooper, H.J., Hudgins, R.R., Hakansson, K., Marshall, A.G.: Characterization of amino acid side chain losses in electron capture dissociation. *J. Am. Soc. Mass Spectrom.* **13**(3), 241–249 (2002)
42. Haselmann, K.F., Budnik, B.A., Kjeldsen, F., Polfer, N.C., Zubarev, R.A.: Can the (M center dot X) region in electron capture dissociation provide reliable information on amino acid composition of polypeptides? *Eur. J. Mass Spectrom.* **8**(6), 461–469 (2002)
43. Fung, Y.M.E., Chan, T.W.D.: Experimental and theoretical investigations of the loss of amino acid side chains in electron capture dissociation of model peptides. *J. Am. Soc. Mass Spectrom.* **16**(9), 1523–1535 (2005)